

---

## ***In Vivo* Recording of Blood Velocity Profiles and Studies *In Vitro* of Profile Alterations Induced by Known Stenoses**

---

**Mario Bassini, Ph.D.,\* Emilio Gatti, Ph.D.,†  
Tito Longo, M.D.,‡ Gianmarco Martinis, Ph.D.,\*  
Paolo Pignoli, M.D.,‡ Pier Luigi Pizzolati, Ph.D.\***

*Recordings of blood velocity profiles and their behavior in the time domain in some peripheral human vessels (carotid arteries and limb vessels) are reported.*

*Measurements have been obtained with a pulsed ultrasonic instrument based on the analysis of the cross-correlation function of blood-diffused echoes. The alterations of blood velocity profiles and of the velocity in the time domain, induced by known stenosis, have been studied in vitro as a function of the distance between stenosis and measuring point, and the position of the sample volume along the diameter. These studies may be useful for a better comprehension of blood velocity measurements made with ultrasound equipment for clinical noninvasive diagnostic purposes.*

**T**HE INTEREST in early atherosclerotic plaque is increasing because of its recognized embolic potential, which manifests in the cerebral circulation by transient ischemic attacks (TIA).<sup>1</sup>

Furthermore, some experimental evidence supports the hypothesis that, in some circumstances, early atherosclerotic plaques may regress.<sup>2</sup> However, the detection of these important lesions is a challenging problem because they do not reduce pressure and flow distally, and they are not detectable by simple means (pressure and flow measurements), as are the more advanced stage (lumen area reduction of 80% or more) hemodynamically significant stenoses.<sup>3</sup> Biplane contrast angiography has been the most reliable method to diag-

nose these early plaques. The invasiveness of this procedure, however, has many drawbacks. Ultrasonic techniques such as B-mode real time echography,<sup>4</sup> Doppler imaging,<sup>5</sup> and spectral analysis of the pulsed Doppler signal<sup>6</sup> are noninvasive and promise an important diagnostic potential. Because of their low calcium content, early atherosclerotic plaques show an acoustic impedance quite similar to that of blood.<sup>7</sup> This has caused a high incidence of false negatives (more than 50%) in series where B-mode real time echography was used to detect these lesions.<sup>8</sup>

Therefore, the only way in which we can detect the presence and extent of early lesions is through evaluation of the hemodynamic alterations induced within a few

---

*From CISE SpA, Electronics Department, Milan, Italy,\* Politecnico di Milano, Istituto di Fisica, Milan, Italy,† and the Università degli Studi di Milano, Cattedra di Semeiotica Chirurgica I, Policlinico di Milano, Milan, Italy.‡*

*Work supported by CNR/CISE Contract (Milan, Italy).*

---

*Address for reprints: Mario Bassini, Ph.D., CISE SpA, Electronics Department, P.O. Box 12081, 200100 Milan, Italy.*

---

diameters from the plaques.<sup>9</sup> The spectral analysis of the pulsed Doppler signal gives information about the presence and extent of disturbed (turbulent) flow, which has been demonstrated to occur downstream of a 30% (lumen area reduction) symmetric stenosis in the dog's thoracic aorta.<sup>10</sup> In this preliminary report, the changes of velocity profile induced by a known stenosis *in vitro* were measured with an original ultrasonic instrument, which differs from current pulsed Doppler velocimeters. This study was undertaken to evaluate the diagnostic potential of the blood velocity profile, which, as far as we know, has not been extensively studied.

## Materials and Methods

### The Flowmeter

Owing to its noninvasive feature, the ultrasonic technique for measuring blood flow *in vivo* has been widely accepted as a diagnostic tool. Ultrasonic energy can be transmitted towards the vessels, either as a continuous wave or as a pulsed wavetrain. The former technique provides a blood velocity measurement averaged over the ultrasound path; the latter technique gives a value relevant to a limited portion of the beam, when range gating is applied to the received echo; however, both methods evaluate the velocity of measuring Doppler frequency shifts.

A different approach, based on correlation functions (presented in preliminary works<sup>11,12</sup>) has been developed. In the following sections, the performance of this new method is described and compared to the pulsed Doppler technique.

**The working principle.** A short voltage pulse is applied to a wideband ultrasound transducer so that a short pressure pulse travels in a narrow beam through the medium, acoustically coupled to the transducer. Each inhomogeneity within the beam backscatters some acoustical energy; the transducer, operated in receiving mode, gives an electrical signal which is a

time version of the medium structure along the beam. If the medium undergoes a movement in the direction of the beam, the output signals (corresponding to successive pulses) exhibit time displacements (Fig. 1A) proportional to the medium velocity; the medium velocity can be measured by calculating the correlation function between successive echoes (Fig. 1B). The velocity at a definite depth can be measured by processing a selected part of the received signal.

In the presence of medium movement that is not parallel to the beam axis, only the velocity projection along the beam is measured; however, the transverse component of the velocity reduces the correlation between the signals, introducing some noise. In Figure 2, the scheme of the measurement and the relevant mathematical relationship are illustrated.

**Flowmeter description.** An instrument which allows recording of velocity profiles has been realized: its electronic circuitry

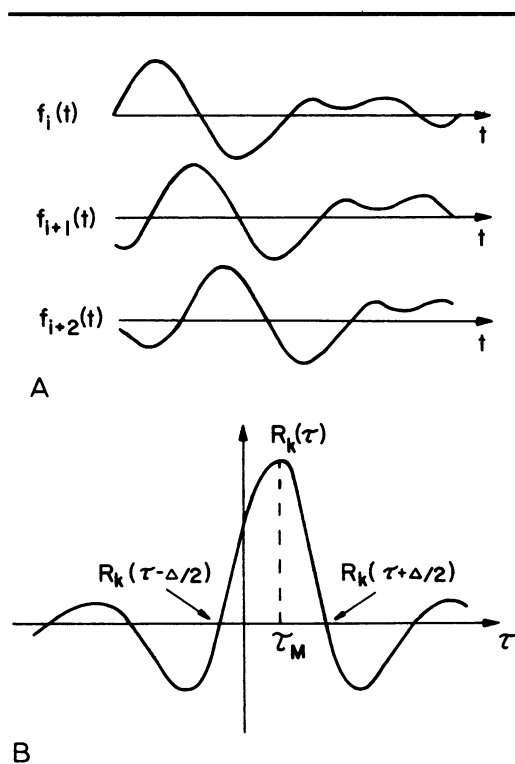


**Fig. 1** Consecutive echoes (a) and their cross-correlation function (b).

basically consists of a feedback loop that automatically tracks the maximum of the range-gated cross-correlation function. A block diagram of the flowmeter shows how these operations are implemented (Fig. 3). Two points of the cross-correlation function are calculated. The time distance between the echoes chosen for correlation is a selectable number ( $k$ ) of periods of the repetition frequency. This function has the same shape of the autocorrelation function of the echo, but is shifted in time by an amount ( $\tau_M$ ) proportional to the medium velocity.

The time interval ( $\Delta$ ) between the two evaluated points equals half the period of the correlation function (this period is the inverse of the transducer resonating frequency). The automatic tracking system evaluates the function:

$$\phi(\tau) = R_k\left(\tau + \frac{\Delta}{2}\right) - R_k\left(\tau - \frac{\Delta}{2}\right)$$

where  $R_k(\tau)$  is the correlation function, so that  $\phi(\tau) = 0$ . This condition is satisfied when  $\tau = \tau_M$ , and the value of  $\tau$ , which is stored in a register, is continuously updated and available for recording. In Figure 1B, the two calculated points of the correlation are shown in correct tracking condition. With regard to Figure 3, the block  $S_0$  samples the sign of the received echo at time  $t_0$  while  $S_1$  and  $S_2$  sample it at times

$$t_0 + kT + \tau + \frac{\Delta}{2}$$

and

$$t_0 + kT + \tau - \frac{\Delta}{2}$$

respectively, where  $T$  is the ultrasound burst repetition period: the estimation of  $\phi(\tau)$  is obtained by averaging successive  $S_0S_1$  and  $S_0S_2$  products. Part of the sampling circuits are three differential stages that subtract from the signal its average value; any echo arising from fixed structures is then suppressed if it is really stable. Slowly variable echoes from quasi-fixed structures (for example, vessel walls) are a major problem,

because they are not distinguishable from echoes of slowly moving blood.

Actually, this problem is common to all ultrasonic flowmeters (including pulsed Doppler) and a compromise solution must be adopted, choosing a suitable frequency as the boundary between fixed echoes and moving ones.

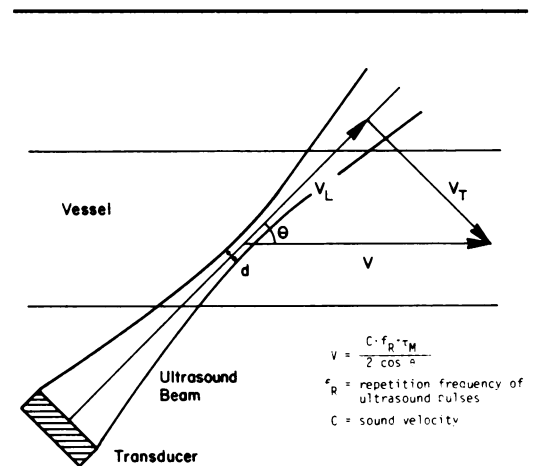


Fig. 2 Transducer geometry and notations.

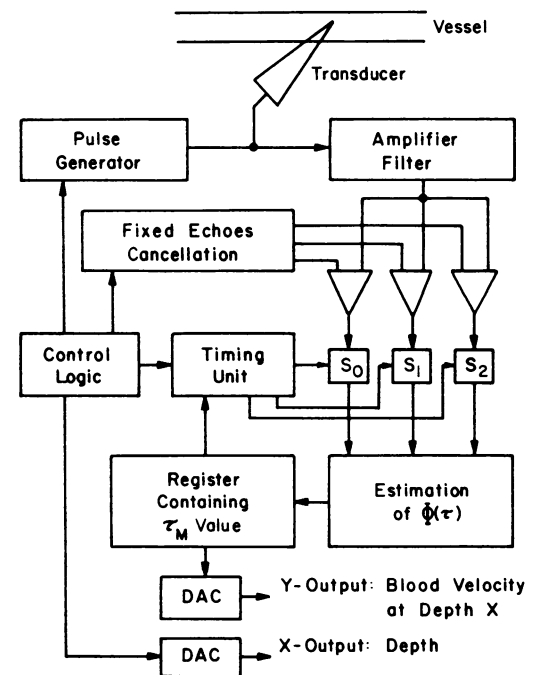


Fig. 3 Flowmeter block diagram,  $S_0, S_1, S_2$  = sampling units.

The value of  $\tau_M$  is related to the velocity by the following equation:

$$\tau_M = \frac{2kV_L T}{C}$$

where:

- $V_L$  = velocity along the transducer axis
- $T$  = pulse repetition period
- $C$  = velocity of the sound in the medium

In order to keep  $\tau_M$  value within the range  $\pm \frac{1}{4f_0}$  (where  $f_0$  is the transducer frequency), suitable values of  $k$  must be chosen, depending on the expected velocity range. The choice, when possible, of  $k > 1$  improves output signal to noise ratio.

**Flowmeter performance.** At present, the flowmeter is equipped with a 6 MHz frequency 3.6 cm focal length transducer, and can obtain the following performances:

- Maximum measuring depth: 4.5 cm
- Spatial resolution: 0.5 mm
- Field depth:  $\approx 1$  cm
- Minimum detectable velocity:  $\approx 1$  cm/sec
- Maximum measurable velocity:  $\approx 120$  cm/sec ( $\theta = 60^\circ$ )
- Pulse repetition rate: 10 KHz
- Time response: the system is able to track a maximum acceleration of 800 cm/sec<sup>2</sup> ( $\theta = 60^\circ$ )
- Profile scan speed: selectable between 0.045 cm/sec and 0.75 mm/sec

The system can be equipped with transducers having frequencies ranging from 2 to 10 MHz; the performances vary according to the chosen transducer.

### Theoretical Comparison with the Doppler System

A theoretical comparison between the performances of our flowmeter and those of a pulsed Doppler system has been implemented under the following assumptions:

- Steady flow
- Constant velocity within the sample volume
- Gaussian intensity distribution of the ultrasound beam at the focus of the transducer
- Absence of echoes from vessel walls

Apart from a small factor caused by sampling the sign only, instead of the entire value of each echo, the variance of the measured velocity appears to be very similar in both methods when measuring high blood velocities.

For moderate and low velocities, better performances are expected by our system due to the possibility of correlating echoes whose time distance is more than one period of the pulse repetition frequency.

### Experimental Set-Up

To obtain good results in a reasonable time, an experimental set-up has been implemented that includes:

- The flowmeter
- A mechanical B-scan
- A pulsed Doppler with audio output
- A minicomputer for off-line reconstruction of profile time behavior

The mechanical B-scan is obtained by moving the transducer of the flowmeter; once the vessel has been localized, the velocity measurement is performed without repositioning the transducer.

The Doppler signal is obtained by synchronous sampling of the return echo and suitable filtering. Both B-scan and audio Doppler are used to quickly identify the vessel. Calibration tests have shown an agreement within 5% by using a timed collection method as a standard.

A minicomputer is connected to the flowmeter. The computer is triggered by the R wave of an electrocardiogram, or by a suitable signal during *in-vitro* measurements, and records the velocity vs time in one point of the vessel. At the next trigger,

the measuring point is shifted by 0.15 mm and a new measure is done, and is so continued. At the end of the acquisition phase, which requires 32 heart cycles, the computer simultaneously displays on a video terminal the velocity profiles vs time and the velocity vs time for every point of the profile. It is also possible to obtain spatial and temporal averages of the profiles to reduce the statistical variance of records.

To test the clinical feasibility of velocity profile measurement by means of the previously described flowmeter, some peripheral vessels have been studied. Figures 4 and 5 show, respectively, the recordings of velocity profiles in the cephalic vein and in two locations of the normal common carotid artery. Figure 6 shows the midstream time behavior of blood velocity in the normal common and internal carotid arteries. In Figure 7, the time evolution of the velocity profile of a normal common carotid artery is reported.

### Hydraulic Model

*In-vitro* measurements of velocity profiles by means of the previously described ultrasonic velocimeter, were performed at various locations with respect to a non-symmetric sharp-edged stenosis (Fig. 10). The induced lumen area reduction was 33%. The hydraulic model, implemented to sim-

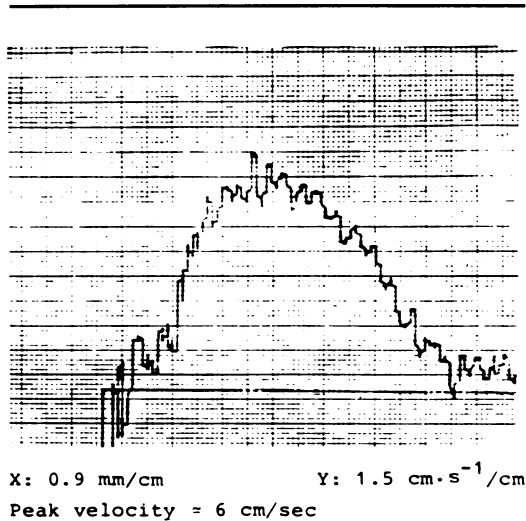


Fig. 4 Velocity profile recorded in a cephalic vein.

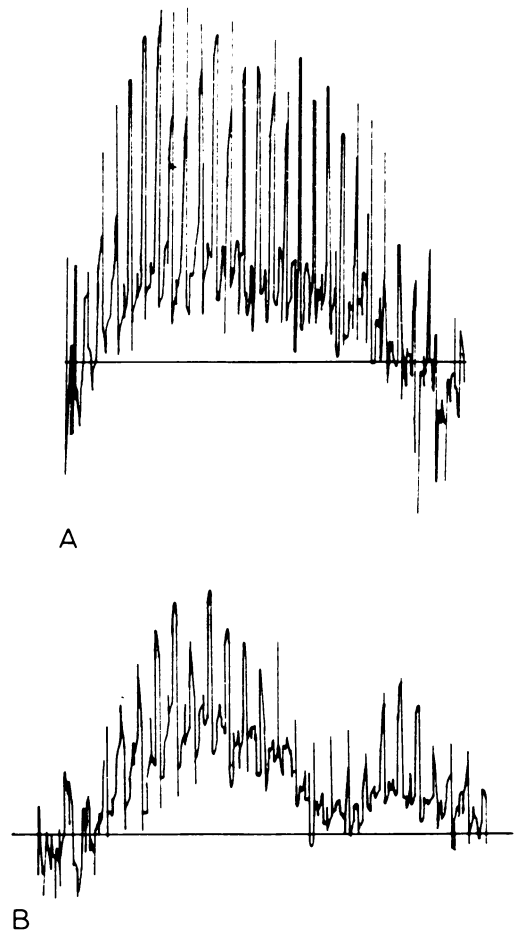


Fig. 5 Velocity profiles recorded in a common carotid artery: (a) proximal location, (b) in the bulb.

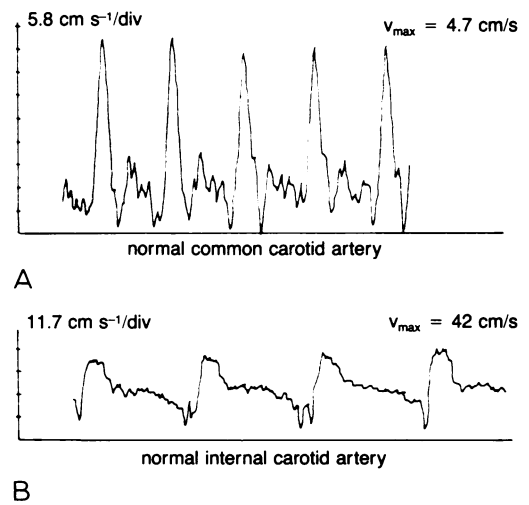


Fig. 6 Blood velocity vs time in the midstream of a common (a) and an internal (b) carotid artery.

ulate the flow pattern of the human common carotid artery (Fig. 8) is schematically represented in Figure 9. Two plexiglass parallel pipes (2.5 meters long), one stenosis-free for reference and the other with the stenosis, ensure the development of a parabolic profile. We used citrated calf blood at room temperature ( $22 \pm 3^\circ\text{C}$ ); the hematocrit was 45%, viscosity 0.05 poise, and RBC diameter  $5 \mu\text{m}$ ; smears of the blood were done before and after several hours of experiments to verify the absence of gross RBC abnormalities and microaggregates. In Table I, some hydraulic parameters characterizing the model are shown.

Velocity profiles were measured in the plane *a* (Fig. 10) at 2 and 1 diameter proximal to the stenosis (2 D-P, 1 D-P), at its center (0-D), and at the 1, 2, 3, and 4 diameter downstream (1D-D, 2D-D, 3D-D, 4D-D).

### Results

At location 0-D, the velocity profile (Fig. 11) permitted measurement of the reduction in vessel diameter due to the 33% non-symmetrical sharp-edged stenosis. The measured residual diameter was  $5.4 \pm 0.4$  mm, whereas, the actual residual diameter was  $5.4 \pm 0.1$  mm. The quoted error on the measured residual diameter was determined by the finite size of the sample volume (0.5 mm) and by inaccuracies of measurement of blood velocities near the walls, due to boundary errors. In a 33% sharp-edged stenosis at 0-D location, the velocity gradients near the walls increased with respect to the 2 P-D values with a flattening of the velocity profile shape. The maximum slope was measured on the side of the profile facing the stenosis. The peak velocities at 0-D and 2 D-P locations were nearly equal; this could be explained by the flattening of the velocity profile, which accounts for the same flow at both locations.

The peak velocity reached its maximum value at 1 D-D location, and at the 4 D-D location, it was still higher than prestenotic (2 P-D) values.

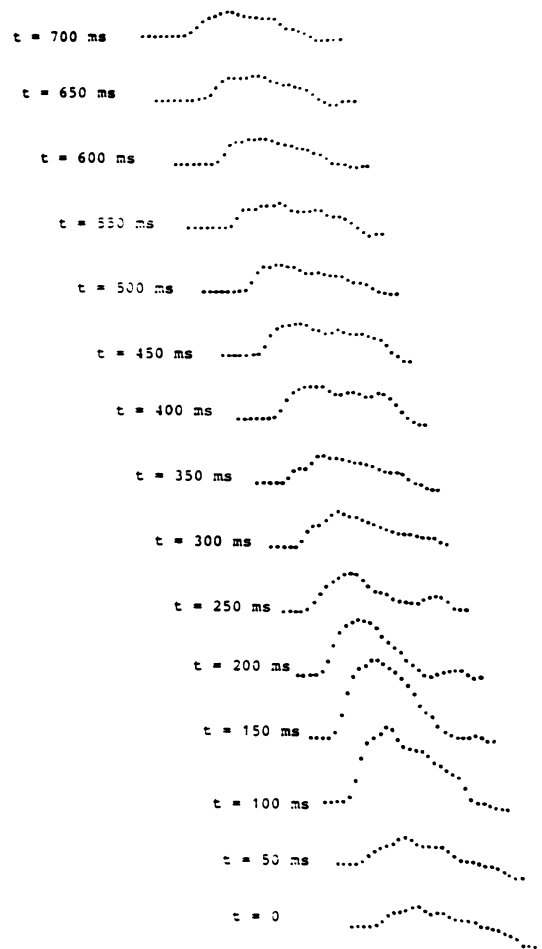


Fig. 7 Time evolution of the velocity profile during cardiac cycle in a common carotid artery.

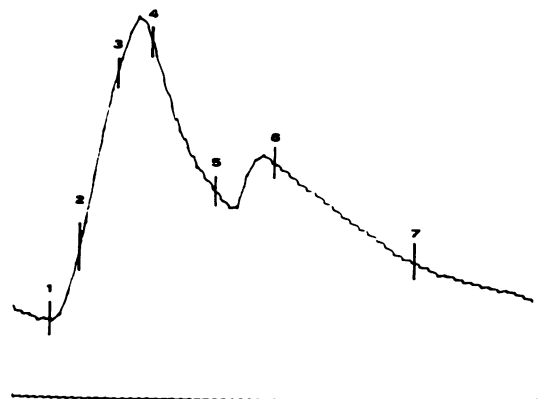


Fig. 8 Blood velocity vs time in the hydraulic model simulating human carotid artery.

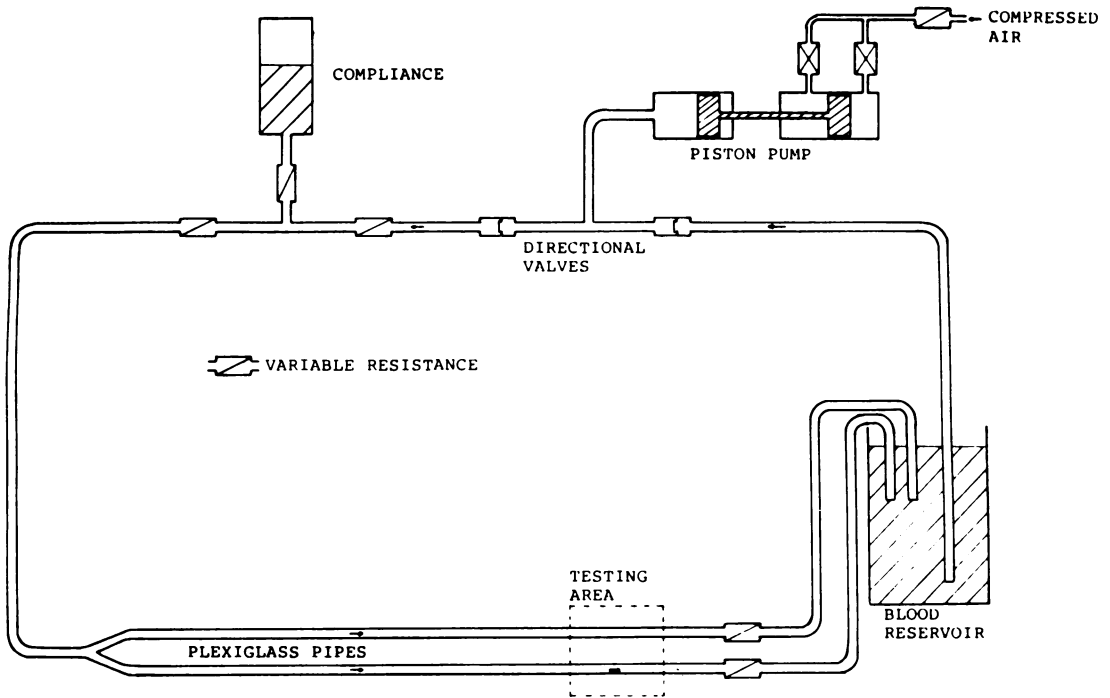


Fig. 9 Hydraulic model simulating blood flow of human carotid artery.

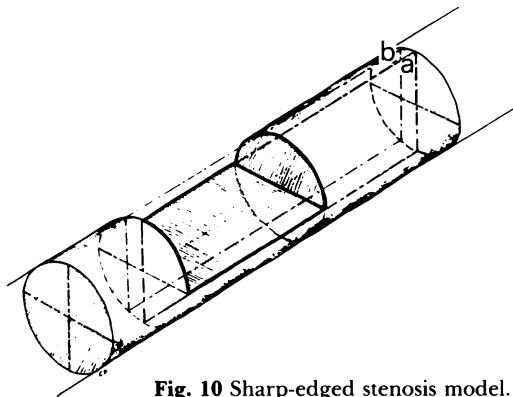


Fig. 10 Sharp-edged stenosis model.

TABLE I. Hydraulic Model Characteristics

Plexiglass pipe internal diameter: 8 mm
Pipe length before the stenosis: 2.5 m
Pulse frequency: 1.13 Hz.
Used fluid: calf blood (Ht 45%, RBC diameter 5 $\mu\text{m}$ , $\mu = 0.05 \text{ p}$ ).
Time and diameter averaged velocity: 30 cm/sec ( $V_{\text{dta}}$ ).
Reynolds number for $V_{\text{dta}} = 400$ .
Kinematic similarity parameters: $\alpha = 4.5$ .
Used stenosis: sharp-edged, non-axisymmetric length: 20 mm, 33% lumen area reducing.

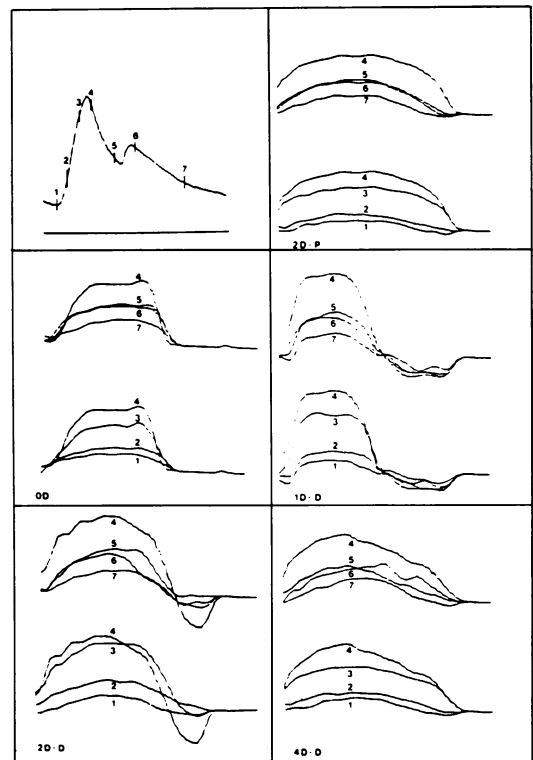


Fig. 11 Velocity profiles vs time at various locations in a model of a 33% sharp-edged stenosis.

The discrete number of measurements we have done does not permit us to extend our knowledge about velocity behavior at points other than those measured. Downstream of the stenosis, the velocity profile showed a reverse flow component, located just behind the stenosis. The magnitude and time behavior of this reverse flow component depended on the distance of the measuring point from the stenosis. The reverse flow began at 1 D-D, reached its maximum at 2 D-D, and had almost entirely disappeared at 4 D-D; however, the velocity profile was still asymmetric with respect to its 2 P-D shape. In the time domain, the reverse flow component was maximum at each location during the early systolic deceleration phase, corresponding to point 4 in Figure 8.

### Discussion

We performed our measurements on a hydraulic model that permitted us to better characterize the geometry of the stenosis, as well as other hemodynamic parameters. Other investigators<sup>13-15</sup> evaluated the velocity profiles induced by smooth-edged axisymmetric stenosis both *in vitro* and *in vivo*. Due to the fact that the geometry of the stenosis and the induced percent area reduction are important in the quantitative evaluation of flow characteristics,<sup>16</sup> we investigated in rigid pipes the behavior of a sharp-edged nonsymmetric stenosis, which is not accurately reproducible in compliant living arteries. The stenoses we evaluated are simplified models (such as the axisymmetrical ones used by other investigators), which approximate the complicated geometries of natural atherosclerotic lesions. *This approximation must be taken into account when transferring the results of these studies to the clinical setting.*

To reduce the differences between the model and the *in vivo* conditions, we produced a pulsatile flow characterized by a waveform similar to the one we registered in the common and internal carotid arteries, which have a so-called resistive flow pattern,<sup>17</sup> i.e., without a reverse flow com-

ponent. As we experienced (and it is predictable from the theoretical analysis<sup>18</sup>), different flow waveforms produce different velocity profiles. The flows previously investigated were steady,<sup>14,15</sup> oscillatory<sup>15</sup> and pulsatile<sup>13</sup>; this last was obtained by superimposing an oscillatory pressure on a mean pressure. We used fresh calf blood, which is supposed to have rheologic properties similar to those of human blood. As the flow waveform and the rheologic properties of the fluid are different from those operating *in vivo*, some uncertainties are supposed to be encountered in the process of transferring the *in-vitro* results to the *in-vivo* setting. Hestand<sup>13</sup> found a good correlation between dog femoral artery velocity profiles and those measured in a model, where the physiologic flow was simulated by controlling the value of the Reynolds number and the kinematic similarity parameter.<sup>18</sup>

The ultrasonic transducer holder may have introduced some errors in the velocity profile measurements, because the position of the transducer along the longitudinal axis of the pipe was determinable with an accuracy of  $\pm 0.25$  diameter and the angulation of the beam was defined with an accuracy of  $\pm 3^\circ$ . Efforts are in progress to ameliorate the accuracy of the transducer position and angle sensing system. The error due to inaccuracies in angle determination was systematic; that is, the velocity profile shape did not change with various angles, which influence only the absolute value.

For obvious reasons, the electronic range gating operated along a beam that was not perpendicular to the longitudinal pipe axis. Therefore, we measured the velocity in points that were not in the same cross section. Between the two cross sections, where the first (i.e., proximal to the transducer) and last (i.e., distal to the transducer) points of velocity measurement lie, and there are 4.6 mm. It is possible to avoid this by a mechanical scanning.<sup>13</sup>

The present report refers to measurements of the velocity profile only in one plane, which is the same in which the steno-



sis develops its contour (Fig. 10). A more systematic tridimensional velocity profile measurement program is running in our laboratory by computer data acquisition and processing. A more extensive tridimensional knowledge of the flow field is necessary for flow volume calculations<sup>14</sup> and for diagnostic clinical purposes, where there is much uncertainty about the relative positions of the stenosis and measured velocity profile planes. Only the acquisition of profiles lying in multiple planes permits the identification of the profile most useful for diagnostic purposes.

The flattening of velocity profile at 0-D, without an increase of velocity, and its increase downstream are findings reported by other investigators,<sup>10,13,15</sup> although the various experimental conditions (flow waveforms and stenosis geometry) make the comparison of the results difficult. It is clinically relevant, however, that Strandness found low-grade stenoses (less than 50%) to produce spectral broadening (i.e., turbulence) without elevation of peak velocity, which increased only for more severe stenoses.

Downstream of the stenosis, the velocity profile showed a reverse flow component located just behind the stenosis. It is apparent that a relatively low-grade stenosis (33%) produces a marked reverse flow in the velocity profile, which, therefore, is likely to be a hemodynamic feature very sensitive to stenosis. Further studies have to be carried out to define the minimum degree of stenosis that induces significant velocity profile alterations.

From theoretical considerations,<sup>18</sup> it is apparent that factors other than the locally restricted geometry may affect the velocity profile shape. In a future research program, pulse frequency, blood viscosity and the flow rate must be taken into account to evaluate the specificity of the velocity profile as a diagnostic tool.

Perhaps the time behavior of the velocity profile may give more information than that contained in the peak velocity profile.

According to the experiments performed, to obtain an accurate map of the

residual lumen by means of ultrasound methods for detecting blood flow (ultrasonic arteriography), it is also necessary to plot points where flow is negative for part of the entire cycle duration. Therefore, current ultrasonic arteriographs<sup>5,19</sup> seem to have some inconvenience with respect to this possibility, because they detect as arterial points only those where there is a positive forward flow; points with a negative reverse flow are disregarded as venous.

*In-vivo* velocity profiles have been measured for physiological purposes<sup>20</sup> and to establish the distribution of wall shear stress, which may be of significance in arterial disease.<sup>21</sup> As far as we know, the potential diagnostic value of the velocity profile has been investigated in a clinical setting only by Anliker.<sup>22</sup> He found that the occlusion of the internal carotid artery affects the common carotid artery velocity profile shape, which is also affected by a severe aortic insufficiency.

### Acknowledgments

The authors wish to thank Mr. G. Melzi, Mr. G. Di Paolo, Mr. F. Franceschi, and Mr. M. Megliani for their technical assistance.

### References

1. Moore WS, Hall AD. Importance of emboli from carotid bifurcation in pathogenesis of cerebral ischemic attacks. Arch Surg 1970; 101:708.
2. Wissler RW, Vesselinovitch D. Studies of regression of advanced atherosclerosis in experimental animals and man. Ann NY Acad Sci 1976; 275:363.
3. Berguer R, Hwang NHC. Critical arterial stenosis: A theoretical and experimental solution. Ann Surg 1974; 180:39.
4. Green PS, Taenzer JC, Ramsey SD Jr, Holzemer JF, Suarez JR, Marich KW, Evans TC, Sandok BA, Greenleaf JF. A real-time ultrasonic imaging system for carotid arteriography. Ultrasound Med Biol 1977; 3:129.
5. Mozersky DJ, Hokanson DE, Baker DW, Sumner DS, Strandness DE. Ultrasonic arteriography. Arch Surg 1971; 103:663.
6. Blackshear WM, Phillips DJ, Thiele BL, Hirsch JH, Chikos PM, Marinelli MR, Ward KJ, Strandness DE Jr. Detection of carotid occlusive disease by ultrasonic imaging and pulsed Doppler spectrum analysis. Surgery 1979; 86:698.

7. Hartley CJ, Strandness DE. The effects of atherosclerosis on the transmission of ultrasound. *J Surg Res* 1969; 9:579.
8. Hobson RW II, Berry SM, Katocs AS Jr, O'Donnell JA, Jamil Z, Savitsky JP. Comparison of pulsed Doppler and real-time B-mode echo arteriography for noninvasive imaging of the extracranial carotid arteries. *Circ Res* 1980; 87:286.
9. Giddens DP, Mabon RF, Cassanova RA. Measurement of disordered flows distal to subtotal vascular stenoses in the thoracic aortas of dogs. *Circ Res* 1976; 39:122.
10. Thiele BL, Hutchinson KJ, Bodily FK, Forster FK, Strandness DE. Pulsed Doppler velocity waveform patterns produced by smooth stenoses in the dog thoracic aorta. *Biol Eng Soc Proc*, March 1980, London.
11. Dotti D, Gatti E, Svelto V, Ugge A, Vidali P. Blood flow measurements by ultrasound correlation techniques. *Energia Nucleare* 1976; 23:571.
12. Bassini M, Dotti D, Gatti E, Pizzolati PL, Svelto V. An ultrasonic non-invasive blood flowmeter based on cross-correlation techniques. *Ultrasonic International Proceedings* 1979; Gratz.
13. Green ER, Hstrand MB. Ultrasonic assessment of simulated atherosclerosis: *In vitro* comparisons. *J Biomech Eng* 1979; 101:73.
14. Hagl S, Messmer K, Pfau B, Meisner H. Influence of stenosis on the velocity profile analyzed by a pulsed Doppler ultrasonic flowmeter. In *Cardiovascular Applications of Ultrasound*, Reneman RS (ed). North Holland Publ. Co., The Netherlands 1974; p 216.
15. Peronneau PA, Hinglais JR, Xhaard M, Delouche P, Philippo J. The effects of curvature and stenosis on pulsatile flow *in vivo* and *in vitro*. *Cardiovascular Applications of Ultrasound*, Reneman RS (ed). North Holland Publ. Co., The Netherlands 1974; p 203.
16. Young DF, Tsai FY. Flow characteristics in models of arterial stenoses-II. Unsteady flow. *J Biomech* 1973; 6:547.
17. Spencer MP, Denison AB. Pulsatile blood flow in the vascular system. In *Handbook of Physiology*, Vol. II, Section II, Circulation, p 853, American Physiological Society 1963; Washington, D.C.
18. Hale JF, McDonald DA, Womersley JR. Velocity profiles of oscillating arterial flow, with some calculations of viscous drag and the Reynolds number. *J Physiol* 1955; 128:629.
19. Spencer MP, Reid JM, Davis DL, Paulson BS. Cervical carotid imaging with a continuous wave Doppler flowmeter. *Stroke* 1974; 5:145.
20. Clark C, Schultz DL. Velocity distribution in aortic flow. *Cardiovasc Res* 1973; 7:601.
21. Atabek HB, Ling SC, Patel DJ. Analysis of coronary flow fields in thoracotomized dogs. *Circ Res* 1975; 37:752.
22. Keller HM, Meier WE, Anliker M, Kumpe DA. Non-invasive measurement of velocity profiles and blood flow in the common carotid artery by pulsed Doppler ultrasound. *Stroke* 1976; 7:370.